

The Design and Measurement of Two Broad-Band Coaxial Phase Shifters*

C. F. AUGUSTINE AND J. CHEAL,† MEMBER, IRE

Summary—Two mechanical (servo-driven) phase shifters were developed in response to systems requirements of low torque, compactness, octave bandwidth, and linear relation between mechanical motion and phase shift. One phase shifter relies upon the axial motion of a dielectric slug through a helix wound from modified miniature rigid coaxial cable. The second design consists of a 3-db coupler with ganged movable shorts on two ports. The helix design displayed phase shift of 720 degrees at 3 kmc and linearity to within ± 3 degrees. The coupler design is capable of achieving 720 degrees phase shift at 3 kmc and linearity within ± 2 degrees. A precision measuring facility (phase bridge) was developed for the purpose of determining the electrical performance of the phase shifters. A brief analysis is included to illustrate the prediction of maximum possible errors in the phase bridge and the phase shifters, in terms of transmission line parameters.

INTRODUCTION

TWO phase shifters were developed to meet systems requirements that were unusually demanding both electrically and mechanically. The requirements were essentially as follows:

Electrical:

- 1) Operation in the TEM mode from 2 to 4 kmc.
- 2) Phase shift vs mechanical motion linear to within ± 3 degrees.
- 3) Total phase shift of at least 400 degrees at 3 kmc.
- 4) Insertion loss of less than 3 db.

Mechanical:

- 1) Low torque.
- 2) Small size.
- 3) Rugged construction.
- 4) Simple mechanical motion.

The two designs meet these requirements through novel techniques employed to obtain both the electrical accuracy and the small size.

At the outset of the development program, it was recognized that an accurate test facility would be necessary to determine electrical performance. An S-band phase bridge was designed for this purpose. At the conclusion of this paper, a brief explanation of this phase bridge and an analysis of maximum possible measurement errors are given.

HELICAL PHASE SHIFTER

In this device phase shift is the result of axial motion of a cylindrical slug through a helical transmission line. The slug and transmission line are shown in Fig. 1.

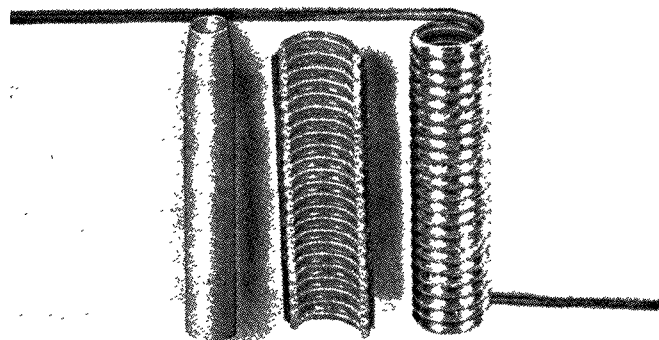


Fig. 1—Helix and dielectric slug.

The slug is comprised of low loss material having a high dielectric constant, and is available under the trade name of Styrofoam. It has a dielectric constant and loss tangent of about 15 and 0.001, respectively, from 2 to 4 kmc.

The helix is 2.25 inches long with an inner diameter of 0.450 inch. It is fabricated from miniature 50-ohm coaxial cable which has an outside diameter of 0.085 inch. The outer shield is solid copper and the center conductor is supported by a solid dielectric of teflon. A portion of this cable is machined away until the center conductor is exposed but still firmly supported by the dielectric. The helix is formed by wrapping the machined coax on a removable cylindrical mandrel and soldering the outer shield of successive turns together.

The cylindrical coax is tapered into the machined coax at both ends of the helix to effect a smooth wide-band electrical transition. The dielectric slug is also tapered to provide a better impedance match. The clearance between the outside diameter of the dielectric slug and the inside diameter of the helix is about 0.002 inch. This clearance must be kept small so that the high dielectric constant material will have maximum effect on the rather weak fringing fields around the exposed center conductors.

Fig. 2 shows how helix and slug are assembled. The helix is potted into the barrel assembly. It is supported during the potting process with a mandrel, which assures that the ID of the helix will remain concentric with the lead-screw bearings. The slug is mounted on the lead screw, which is in turn driven by the servo motor through a gear train.

* Received by the PGM TT, July 31, 1959; revised manuscript received, February 8, 1960. Presented at IRE-PGM TT Nat'l. Symp., Harvard University, Cambridge, Mass., June 1-3, 1959.

† Research Div., Bendix Aviation Corp., Detroit, Mich.

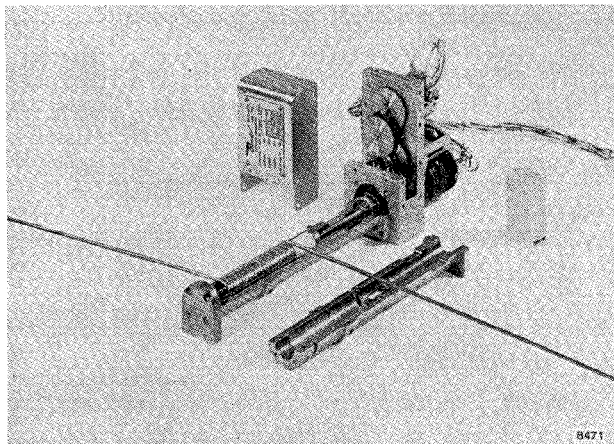


Fig. 2—Partially assembled helical shifter.

A typical curve of the relation between slug penetration into the helix and phase shift is shown in Fig. 3. Total phase shift for 1.8 inches of slug penetration is 490 degrees at 2.97 kmc and is linear to within ± 3 degrees. Maximum insertion loss at 3 kmc is less than 2 db. If lower loss is desired, a slug formed of Alite or an aluminum oxide of equivalent properties would give some improvement over the Styccast. From 2 to 4 kmc, the loss tangent and dielectric constant of this material are about 0.0007 and 8.5, respectively.

The maximum VSWR measured as a function of slug position was 1.5; however, a large portion of this mismatch can be attributed to the input and output connectors. Although the unit was designed to operate primarily over the frequency range of 2 to 4 kmc, the phase shift characteristics were checked at both higher and lower frequencies. Fig. 4 shows a plot of phase shift vs slug travel at 500, 1000, 2000, 4000, and 8000 mc. These curves indicate that the device is usable over this entire range, with total phase shift linearly related to frequency.

Aside from the phase-shifter applications, this helical transmission line has been used for testing ferrites and absorbing material. A compact variable attenuator can be fabricated by inserting a slug of high loss material into the helix.

PHASE SHIFTER USING 3-DB COUPLER

The second type of phase shifter utilizes an operating principle based on the variation of line lengths. Fig. 5 is a schematic representation of this operating principle, which is well-known in connection with waveguide hybrids. Opposite ports of the 3-db coupler are terminated with movable shorts. The terminated line lengths are kept equal by a suitable ganging technique. With equal power split between the two terminated ports, the reflected power is added at the fourth port and cancelled at the input. Phase difference between input and output is then a function of l . In this phase shifter, a change in the short positions by one-half wavelength corresponds to 360 degrees of phase shift.

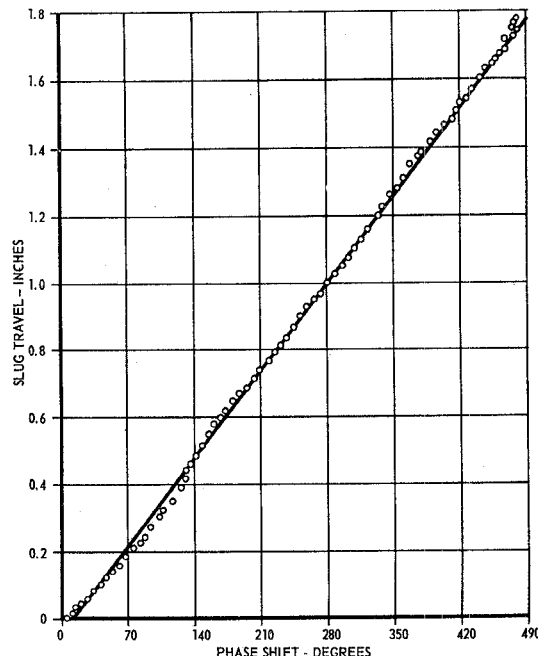


Fig. 3—Phase shift vs slug penetration at 2.97 kmc.

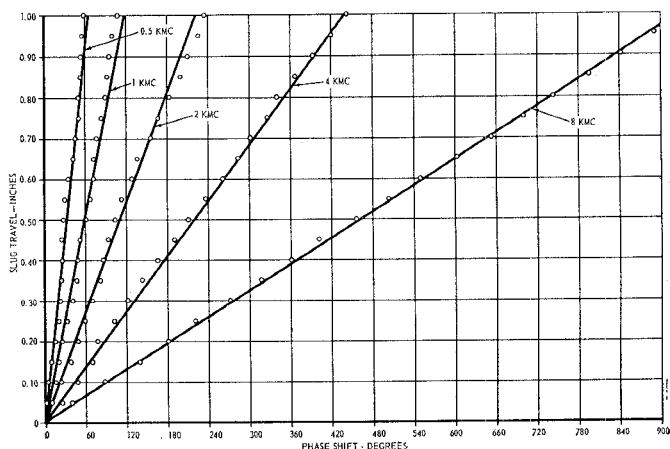


Fig. 4—Phase shift vs slug penetration at various frequencies.

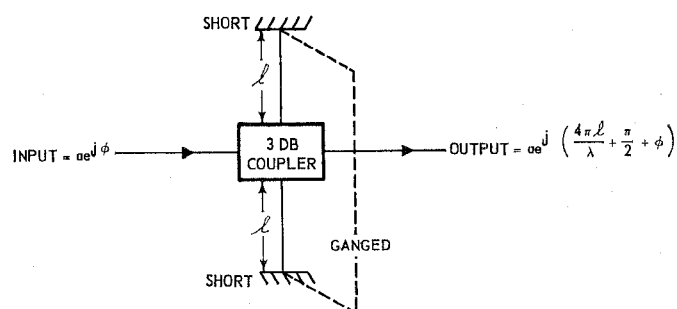


Fig. 5—Relation between input and output

Fig. 6 shows the 3-db coupler with input and output connections. The coaxial leads are brought in through the sides of the housing cylinder. The flat strips in the center of the cylinder form the broadband coupling section and are one-quarter wavelength long at the center of the frequency band. The two ports that are terminated with the movable shorts are brought around on the front side of the cylinder and curved around the outer periphery.

In Fig. 7, the coaxial line is shown with a portion of the cable machined away to expose the inner conductor. A coaxial line having an outside diameter of 0.141 inch is used for this purpose. Sliding contacts short the center conductor to the outer shield, and phase shift is accomplished by a rotary motion of the arm.

The 3-db coupler characteristics are shown in Fig. 8. The coupling is almost exactly 3 db from 2.7 to 3.3

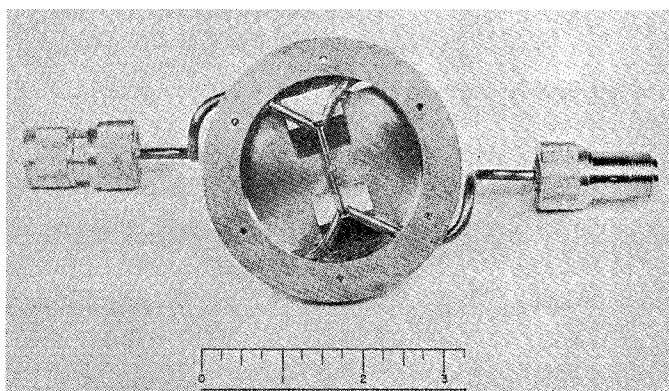


Fig. 6—Rear view showing 3-db coupler.

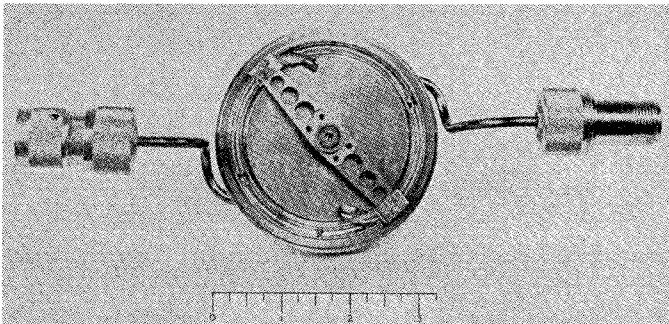


Fig. 7—Front view showing ganged shorts.

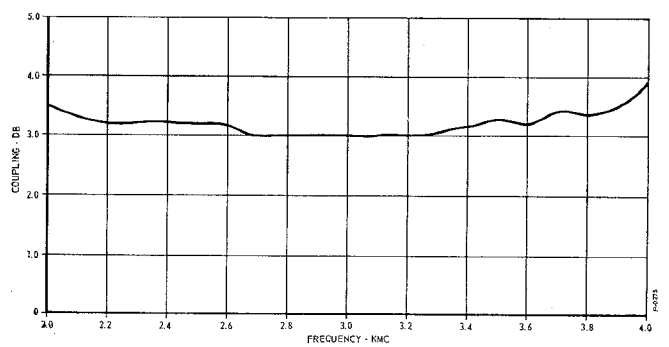


Fig. 8—Characteristics of 3-db coupler.

kmc, and less than 0.5 db deviation was measured from 2 to 3.9 kmc. The slight departure from equal power division will contribute to an impedance mismatch at the input port. The reflected power resulting from this mismatch will not affect the phase linearity if multiple reflections are suppressed with a matched line looking back from the input port. However, any discontinuities in the input line will contribute to phase nonlinearity. For example, if the connector on the input port has a VSWR of 1.2 and the coupling is 3.5 db rather than 3 db, it can be shown that this combination can lead to a maximum deviation from linearity of 2.5 degrees.

The curve relating radial displacement of the ganged shorts to phase shift at 3 kmc is given in Fig. 9. The maximum departure from the linear curve is less than ± 2 degrees.

A complete assembly with speed-reduction gears and servo drive is shown in Fig. 10. The unit is less than 3 inches high, including the servo motor, and is 3.25 inches in diameter.

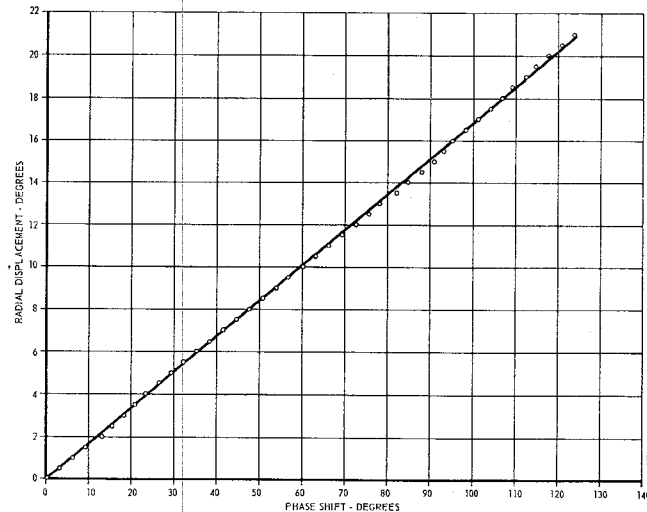


Fig. 9—Phase shift vs radial displacement.

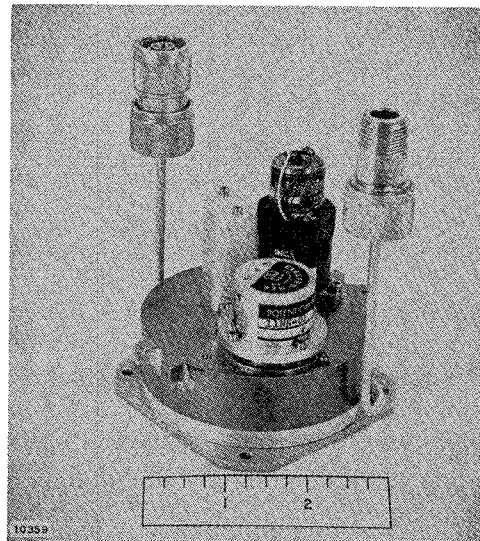


Fig. 10—Complete assembly.

MEASUREMENT TECHNIQUES

As mentioned previously, an *S*-band phase bridge was developed for the measurement of the phase-shifter performance. A block diagram of the bridge is shown in Fig. 11. Bridges of this type are preferred over slotted lines in phase measurement because greater accuracy and resolution can be obtained.

Power division and recombination is accomplished by two 3-db stripline couplers. The standards are commercially-available coaxial line stretchers that have been equipped with a precision mechanical movement. Fixed coaxial attenuators are placed at the inputs and outputs of the line stretchers to guarantee good impedance match at these ports.

There are two principal sources of error in the phase bridge. The first results from the fact that the line-stretcher standards do not face perfect impedances. The other comes about because the device to be measured is inserted between terminals that deviate slightly from the nominal impedance. A simple method of determining maximum possible errors of the first type is illustrated in Fig. 12. The line stretcher is assumed perfect, but there are impedance discontinuities at the input and output terminals resulting in reflection coefficients q_1 and q_2 . These reflection coefficients will cause a departure from linearity in the mechanical displacement vs phase-shift characteristic. The exact magnitude of the departure can be found by adding up all the terms resulting from multiple reflections just to the left of q_2 , dividing by the voltage that would be obtained at this point if q_1 and q_2 were zero, and taking the argument of

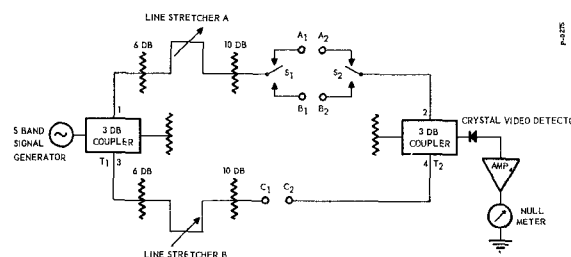
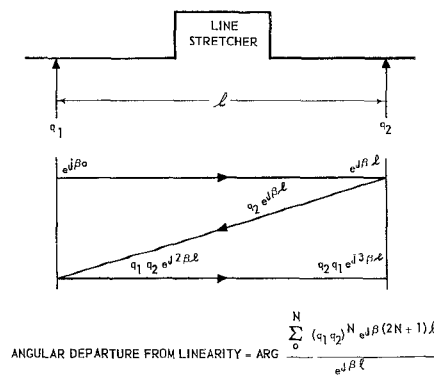
Fig. 11—*S*-band bridge.

Fig. 12—Maximum departure from linearity as a function of two impedance discontinuities.

the complete expression, *i.e.*,

$$\text{angular departure} = \text{ARG} \frac{\sum_0^N (q_1 q_2)^N e^{j\beta(2N+1)l}}{e^{j\beta l}}. \quad (1)$$

For small reflection coefficients, the maximum departure is found with sufficient accuracy as,

$$\text{maximum departure} \simeq \text{arc tan} |q_1| |q_2|. \quad (2)$$

For example, in the line stretchers used in the phase bridge,

$$|q_1| \simeq |q_2| = 0.09,$$

which results in a maximum departure or possible error of ± 0.5 degrees.

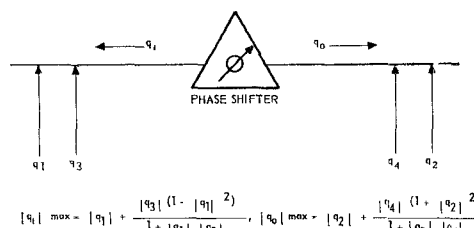
If the discontinuities represented by q_1 and q_2 are part of the phase shifter under consideration (they may, for example, be connectors at the input and outputs), then the deviation just described is not an error but is a part of the performance characteristics. If the device is measured between perfect impedances, there is no question but that a true insertion phase measurement is made. In practice, however, this cannot be the case and confusion may arise since deviation from the expected characteristic is partially due to impedance irregularities at the terminals of the device and partially due to deviations at the terminals of the testing facility. For example, the situation may be as shown in Fig. 13. Reflection coefficients q_3 and q_4 may be due to connectors at the ports of a phase shifter to be tested, and q_1 and q_2 may be reflection coefficients at the ports of the measurement facility. It is possible to have a line length between q_1 and q_3 such that the reflection coefficient q_1 looking back from the phase shifter has a maximum value given by

$$|q_1|_{\max} = |q_1| + \frac{|q_3| (1 + |q_1|^2)}{1 + |q_1| |q_3|}. \quad (3)$$

A similar expression relates q_0 with q_2 and q_4 . When all reflection coefficients are small, the maximum possible error is very nearly given by

maximum possible error

$$\simeq \text{arc tan} |q_1| |q_0| - \text{arc tan} |q_3| |q_4|. \quad (4)$$



$$\text{MAXIMUM POSSIBLE ERROR} \simeq \text{ARC TAN} [|q_1| |q_0|] \cdot \text{ARC TAN} [|q_3| |q_4|]$$

Fig. 13—Maximum possible error caused by impedance deviations at the bridge terminals.

The maximum possible error that can occur during a measurement on a phase bridge is therefore equal to the sum of (2) and (4), and is always a function of the deviation from nominal impedance at the terminals of the device under test. However, it is very unlikely that the line lengths between discontinuities would be arranged so that the error would achieve the maximum possible value during any measurement.

Unequal power division between the two bridge arms will introduce no direct error. However, if the inequality is large enough to decrease appreciably the sharpness of the output null, error may be introduced because of increased uncertainty in the exact setting of the line stretchers.

CONCLUSION

Both phase shifters have the advantage of small physical size, potential rugged construction and linear relation between phase shift and mechanical motion. The low driving torque necessary to accomplish phase

shift is an attractive feature for servo-control applications.

The helical phase shifter has a bandwidth advantage over the coupler type but has a greater insertion loss. The bandwidth of the helix phase shifter extends from UHF up through C band, whereas the bandwidth of the coupler type is limited to less than an octave. However, the linearity of the coupler type is somewhat greater than in the helical phase shifter. Both designs are intended for low-power receiver types of applications, and maximum power-handling capacity has not been determined.

For precise phase measurements, bridge methods are recommended rather than slotted-line techniques. The chief source of measurement error is caused by interactions between impedance deviations at the terminals of the phase shifter and deviations at the terminals of the testing facility. The maximum possible phase errors that can occur as a result of the deviations can be calculated by the methods that have been given.

A Dielectric Resonator Method of Measuring Inductive Capacities in the Millimeter Range*

B. W. HAKKI† AND P. D. COLEMAN†, MEMBER, IRE

Summary—A novel technique for the measurement of dielectric and magnetic properties of a homogeneous isotropic medium in the range of approximately 3 to 100 kmc is described. An accuracy of ± 0.1 per cent is possible in the determination of permittivity or permeability in those cases where the loss tangent is sufficiently small. The measuring structure is a resonator made up of a right circular cylindrical dielectric rod placed between two parallel conducting plates. For measurement of permittivity two or more resonant TE_{onl} mode frequencies are determined whereas for the measurement of permeability two or more resonant TM_{onl} mode frequencies are determined. The dielectric or magnetic properties are computed from the resonance frequencies, structure dimensions, and unloaded Q . Since the loss tangent is inversely proportional to the unloaded Q of the structure, the precision to which Q is measured determines the accuracy of the loss tangent.

I. INTRODUCTION

MOST of the methods for the measurement of dielectric and magnetic properties of materials at microwave frequencies fall into the following

categories: perturbation techniques, optical methods, transmission line methods, or exact resonance methods. The perturbation techniques have notably been used in ferrite measurements where a small piece of the material to be measured, either in the form of a disk or a sphere, is placed in a metallic resonant cavity operating in a known mode and the shift in resonant frequency and the Q of the structure is noted.¹⁻⁴ Optical techniques at microwave frequencies⁵ are inherently suited for measurements below a wavelength of one centimeter, but

¹ W. Von Aulock and J. H. Rowen, "Measurement of dielectric and magnetic properties of ferromagnetic materials at microwave frequencies," *Bell Sys. Tech. J.*, vol. 36, pp. 427-448; March, 1957.

² E. G. Spencer, R. C. LeCraw, and F. Reggia, "Measurement of microwave dielectric constants and tensor permeabilities of ferrite spheres," *Proc. IRE*, vol. 44, pp. 790-800; June, 1956.

³ J. O. Artman and P. E. Tannenwald, "Measurement of permeability tensor in ferrites," *Phys. Rev.*, vol. 91, pp. 1014-1015; August 15, 1953.

⁴ J. O. Artman and P. E. Tannenwald, "Microwave susceptibility measurements in ferrites," *J. Appl. Phys.*, vol. 26, pp. 1124-0000; September, 1955.

⁵ T. E. Talpey, "Optical methods for the measurement of complex dielectric and magnetic constants at centimeter and millimeter wavelengths," *IRE TRANS. ON MICROWAVE THEORY AND TECHNIQUES*, vol. MTT-2, pp. 1-13; September, 1954.

* Received by the PGMTT, December 24, 1959; revised manuscript received, February 15, 1960. This work was sponsored by the U. S. Atomic Energy Commission under Contract No. AT(11-1)-392.

† Elec. Engrg. Res. Lab., University of Illinois, Urbana, Ill.